Elansary *et al.*
Journal of Engineering and Applied Science (2023) 70:70
https://doi.org/10.1186/s44147-023-00243-3

Journal of Engineering and Applied Science

RESEARCH Open Access

Structural system yielding minimum differences between ordinary and staged analyses

Ahmed A. Elansary[1,2*], Mohamed I. Metwally[3,4] and Adel G. El-Attar[5]

*Correspondence:
aelansa2@uwo.ca;
ahmedalaaansary@eng.cu.edu.eg

[1] Department of Structural Engineering, Faculty of Engineering, Cairo University, Giza 12613, Egypt
[2] Department of Civil and Environmental Engineering, Faculty of Engineering, The University of Western Ontario, London, ON N6A3K7, Canada
[3] Department of Structural Engineering, Faculty of Engineering, Horus University, Damietta 34511, Egypt
[4] Mansoura College Academy, Mansoura High Institute of Engineering and Technology, Mansoura 35681, Egypt
[5] Departmen of Structural Engineering, Faculty of Engineering, Cairo University, Giza 12613, Egypt

Abstract

Structural engineers should appropriately design concrete structures to resist lateral loads. Determining the adequate system for resisting the expected lateral loads is important to control the building drift. Choosing the appropriate system is usually conducted assuming the predicted forces are applied to completed concrete buildings at one step which is commonly known as ordinary analysis (*OA*). Nevertheless, these structures are constructed sequentially which requires using staged analysis (*SA*) instead of *OA*. In this paper, a comprehensive numerical model for *SA* of concrete buildings, which accounts for time dependent effects, is utilized using a well-validated commercial software. Six reinforced concrete buildings with 10 and 20 storeys are analyzed using the developed model. Three various structural systems are considered (Rigid Frame (*RF*), Shear Wall (*SW*), and Wall Frame (*WF*). A comparison is conducted between the displacements and internal forces in beams and slabs obtained from the *SA* and *OA*. For a 10-storeys *RF* building, maximum bending moment from *SA* is 29.9% higher than that from *OA*. The same conclusion was observed for the maximum shearing force with a percentage of 19.6%. Moreover, maximum bending moments and shearing forces from SA for the 20-storeys *RF* building are, respectively, 35.0% and 23.5% larger than those from *OA*. The *RF* and *WF* systems provided the minimum difference in differential displacement between the *OA* and *SA* analyses. The *RF* system produced the least differences in internal forces from *OA* and *SA* for all studied buildings.

Keywords: Staged analysis, Ordinary analysis, Concrete building, Rigid frame, Shear wall, Wall frame

Introduction

Selecting appropriate structural system to resist lateral loads (*SSRL*) for reinforced concrete structures is critical due to having various options in practice and because this process significantly affects the construction cost. Among different types of *SSRL*, there is usually one system which can resist wind and earthquake loadings with minimum cost. Structural engineers usually determine the *SSRL* for a building based on the number of storeys, gravity and lateral loads, as well as architectural requirements. However, inadequate selection of *SSRL* for reinforced concrete (*RC*) buildings might cause severe damages or uneconomic solutions. Ordinary analysis (*OA*) is commonly adopted

for concrete structures to select the appropriate SSRL where all design loads are applied simultaneously on the entire building. Different research works indicated that the *OA* is not adequate to analyze the concrete structures [1–11] because the dead load is usually applied on these structures in stages. Staged analysis (*SA*) should be utilized instead of *OA* to appropriately find the deformations and straining actions in these structures.

Many authors explored the selection process of an adequate *SSRL* [12–15] by analyzing various concrete structures having various SSRL. Taranath [12] analyzed a set of rigid frames (*RF*) concrete structures where the lateral loads are resisted by the moment resisting beam-column connections. Using this system was found suitable for concrete buildings with a small number of storeys. Based on the adequate *SSRL*, concrete structures were classified by Gunel and Ilgin [13] who reported that RF and shear walls (*SW*) systems can produce ideal solution for 20 and 30-storeys concrete buildings, respectively. El-leithy [14] also selected the adequate *SSRL* by limiting the wind drift for various building heights using ETABS [16]. Likewise, Gunel and Ilgin [13] and El-leithy [14] recommended that *RF* system is adequate for 20-storeys or less concrete buildings. The same limit was recommended for the SW system and extended to 40 storeys for *RC* buildings with *WF* system where the lateral loads are resisted through the interaction between the walls and frames.

However, Katkhoda and Knaa [15] recommended adopting the *WF* system for *RC* residential buildings consisting of 10 to 20 storeys. The authors reached this conclusion after performing the structural design of a number of concrete buildings using an advanced optimization technique. Multiple cycles of analysis and design were performed to determine the minimum cross-sectional dimensions for all reinforced concrete elements of the studied buildings. The obtained solutions achieved significant savings in concrete and steel amounts and consequently the minimum materials cost was obtained. The recommendations by [12–15] were developed based on *OA* but were not validated if *SA* was adopted.

SA should be adopted instead of *OA* to accurately capture the behaviour of *RC* tall buildings [1–11]. Liu et al. [1] assessed structural performance of tall buildings by developing a performance based structural design methodology to control different structural states in various construction stages. The buildings were reported to potentially suffer from safety hazards if the construction stages are ignored in the analysis of tall buildings. The proposed methodology was illustrated by modelling of various tall buildings. The study revealed that *SA* yielded feasible and effective design for tall buildings.

The effect of *SA* was experimentally measured by Su et al. [2] who monitored floor settlements during construction of real buildings. The authors monitored settlement of tall *RC* buildings using *SA*. It was expected that using the developed approach would accurately predict the elevation of the studied building.

Fan et al. [3] used finite element (*FE*) models to estimate the downward displacements during the construction of buildings with a large number of storeys. The investigation was conducted on three super high-rise buildings in China. The study revealed that *OA* yielded relative and total vertical displacements as well as straining actions significantly different from *SA*. Samarakkody et al. [4] studied the effect of differential axial shortening on the behaviour of tall buildings with concrete filled tube (*CFT*) columns. A comprehensive technique was developed and validated for differential axial shortening

(*DAS*) estimation in tall buildings with composite *CFTs*. The study concluded that maximum *DAS*, usually occurs at mid height of the building, can be shifted to the upper floor levels due to considering creep and shrinkage effects. Significant reduction in *DAS* of the vertical load bearing structural components occurred due to introducing an outrigger system. It was shown that using *CFT* in buildings reduced the adverse effects of *DAS*. Correia and Lobo [5] proposed a simplified method to analyze a 45-storeys building with *RF* and central core. The same building was analyzed using the nonlinear staged-construction analysis package offered by the SAP2000 software [17]. The authors found that the internal forces in interior beams of top floors obtained from the proposed simplified method were smaller than their counterparts obtained from the numerical model by 37% and 60% at levels 30 and 40, respectively.

Different researchers showed that time dependent effects should be included in the analysis of *RC* building to adequately evaluate the column shortenings [6–11, 18]. Yang et al. [6] developed and validated a neural network technique to estimate vertical displacements in high-rise concrete buildings. The validation was conducted by comparing the numerical results with those measured experimentally for existing buildings. The developed technique provided more accurate results than conventional numerical models. Moragaspitiya et al. [7] developed a general numerical technique based on finite element modelling, to estimate differential axial shortening in *RC* buildings taking into account the construction sequence. The authors reported that differential axial shortenings might significantly increase due to time dependent effects of concrete. The developed technique was validated by modelling a 64 storey *RC* building. The study concluded that differential axial shortening between perimeter columns were influenced by the axial stiffness of the columns based on load tributary on each column.

Shrinkage, creep and temperature were found critical in evaluating the axial shortening of *RC* shear walls in tall buildings in the construction stage [8]. It was reported that the rate of shrinkage development between columns and shear walls can be significantly different even for elements with same volume–surface ratio. The authors studied the influence of seasonal variation of ambient relative humidity on the shrinkage and creep development of concrete. It was recommended that more experimental studies should be conducted to study the shape effect between prismatic or cylindrical specimens and shear walls. Kwak and Kim [9] analyzed a 10-storey *RC* building to investigate the differences in structural responses between *OA* and *SA* using a numerical model considering time dependent effects of concrete. A verification was conducted by comparing the numerical results with those obtained from previous experiments. The geometric non-linearity and the nonlinear behaviour of concrete were considered. The study concluded that *SA* might produce differential column shortenings and bending moments greater than those obtained from *OA*. These differences were reported to cause serviceability concerns in the non-structural members located between interior and exterior columns. Elansary et al. [10] developed and validated a *FE* model for sequential analysis of concrete buildings and accounted for time dependent effects. Displacements, bending moments, and shear forces from *SA* and *OA* were compared. Displacements from *SA* were larger than those from *OA* by 116% ~ 154% for buildings with various *SSRL*. Performance of post-tensioned (*PT*) slabs in buildings was investigated by Elansary

et al. [11] considering *SA*. Significant differences were detected between the service and ultimate moments, service tensile stresses, slab pre-compression, as well as punching stress obtained from *SA* and *OA*.

Methods

Motivated by the lack of research on selecting the *SSRL* for *RC* building that yields the minimum differences between *OA* and *SA*, this paper has the following objectives. The first is to utilize a comprehensive numerical model to estimate the differences in deformations and straining actions between *OA* and *SA* for two *RC* buildings with three different *SSRL*. The comparison includes differential displacement in vertical members, moments and shear forces in beams, as well as moments in slabs. The second objective is determining the *SSRL* that provides minimum differences between deformations and straining actions obtained from *OA* and *SA* for the investigated buildings. Some essential analysis assumptions, including dimensions, reinforcement, and material properties, are first reported. After that, details of the utilized finite element model (*FEM*) including description of the meshing and time dependent parameters are presented. Then, the settlements, shearing forces and bending moments from *SA* and *OA* are compared. Finally, the authors reported the *SSRL* which provides minimum differences between *OA* and *SA* for each building height.

Basic assumptions

Figure 1 shows 3D views of six different reinforced concrete buildings (B_{d1}, B_{d2}, ... B_{d6}) which have a floor height of 3.5 m and various SSRL, as shown in Fig. 2. Details of the six buildings are presented in Table 1 while concrete dimensions of all structural elements are provided in Table 2. Figure 3 shows that the footprint of the six buildings has dimensions of 30×30 m and a central 6×6 m opening. A thickness of 300 mm is assumed for all slabs to fulfill the deflection regulations. El-leithy [14] estimated the concrete dimensions and reinforcement of the investigated buildings, according to the ACI 318R-05 [19] and the ASCE/SEI 7–05 [20] codes. No change was applied on the cross sections of the column and wall within each five successive floors. Gravity loads (dead and live) as well as wind lateral load (wind speed of 100 mph) were considered in the design [14] where *OA* was adopted. The structural design under seismic loads was also checked according to the ACI 318R-05 [19] and the ASCE/SEI 7–05 [20]. More details of the loading criteria, including partitions, finishing, cladding, live, and wind load, can be found in [14].

The concrete characteristic strength ($f_c^{'}$), Poisson's ratio (υ_c), and Young's modulus (E_c) are 40 MPa, 0.2, and 29,725 MPa, respectively. While the steel yielding stress (f_y), ultimate stress (f_u), Poisson's ratio (υ_s), and Young's modulus (E_s) are 400 MPa, 520 MPa, 0.3 and 200,000 MPa, respectively. Parameters for the shrinkage and creep of concrete are evaluated according to the CEB-FIP [26]. To consider cracking, stiffness for slabs, beams, columns, and walls were reduced by 25, 35, 70, and 70%, respectively. Fixed supports were assigned at the column-foundation connections.

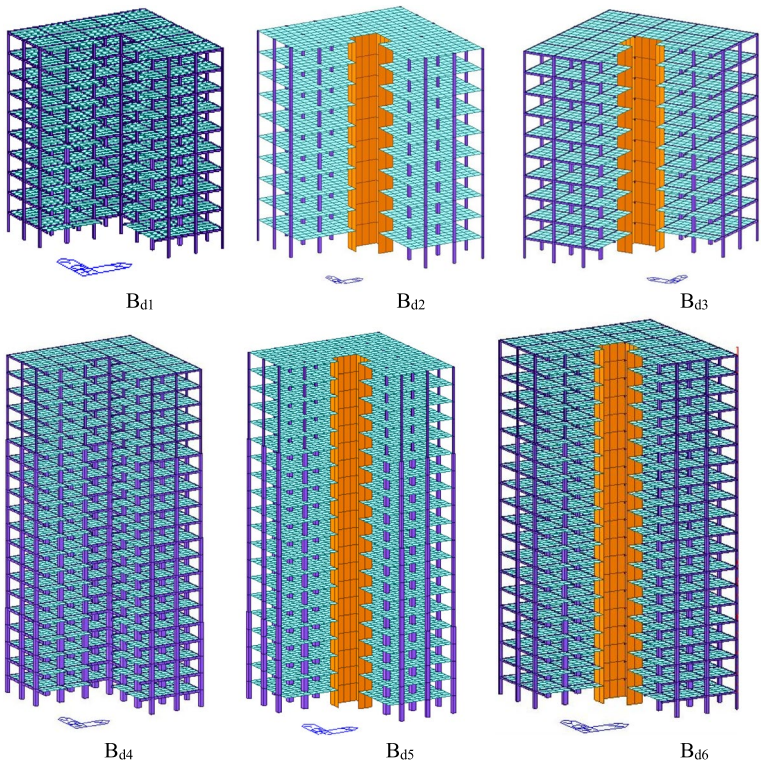

Fig. 1 Three-dimensional view of studied buildings

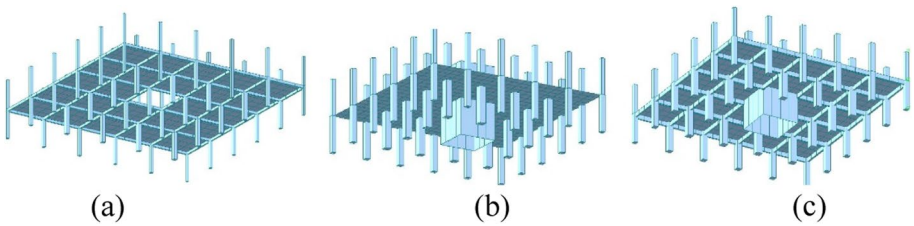

Fig. 2 *SSRL* in the studied buildings

Table 1 Number of storeys, height, and structural system of the investigated buildings

Building designation	No. of storeys	Height (m)	*SSRL*
B_{d1}	10	35	*RF*
B_{d2}	10	35	*SW*
B_{d3}	10	35	*WF*
B_{d4}	20	70	*RF*
B_{d5}	20	70	*SW*
B_{d6}	20	70	*WF*

Numerical modelling

A 3D model is utilized to analyze the investigated concrete buildings using a robust finite element software (midas Gen [21]) which is selected due to the proven efficient

Table 2 Concrete dimensions of structural elements for the investigated buildings (in cm)

Building	Groups[a]	Columns[b]						Core	Beams
		Corner	Edge		Internal				
		C1	C2	C3	C4	C5	C6		
B_{d1}	1	30	40	40	55	55	45		20 × 30
	2	30	40	40	40	40	35		20 × 30
B_{d2}	1	30	40	40	55	55		20	
	2	30	40	40	40	40		20	
B_{d3}	1	30	40	40	55	50		20	20 × 30
	2	30	40	40	40	40		20	20 × 30
B_{d4}	1	70	80	80	105	105	95		20 × 50
	2	60	70	70	85	85	75		20 × 45
	3	50	60	60	75	75	70		20 × 40
	4	30	30	30	45	45	40		20 × 30
B_{d5}	1	70	80	80	105	105		40	
	2	60	70	70	85	85		30	
	3	50	60	60	75	75		20	
	4	30	30	30	45	45		20	
B_{d6}	1	40	55	55	75	75		20	20 × 30
	2	35	45	50	65	65		20	20 × 30
	3	30	40	40	50	50		20	20 × 30
	4	30	30	30	40	35		20	20 × 30

[a] Represents dimensions for structural elements in five successive storeys from base to top of the building

[b] All columns have square cross section

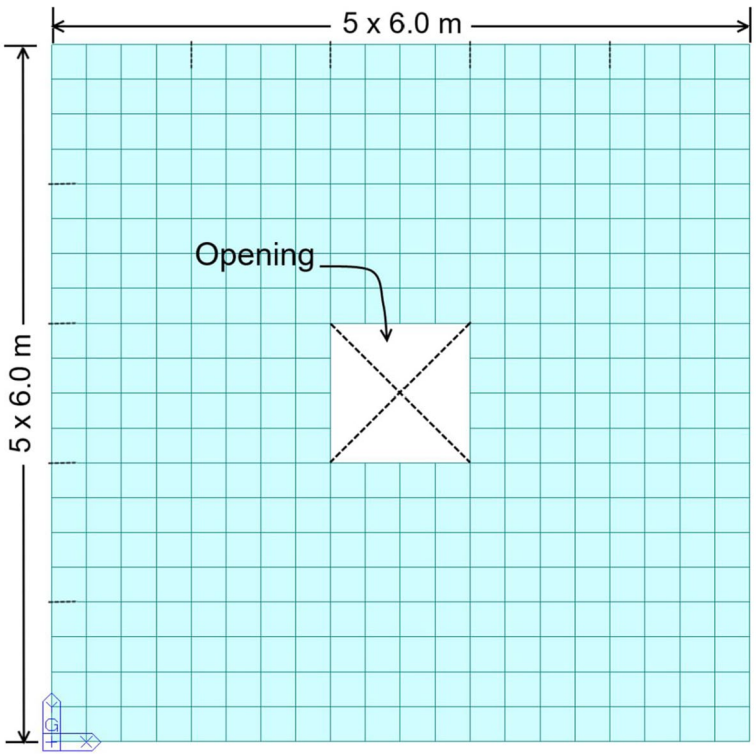

Fig. 3 Plan view of the studied buildings [14]

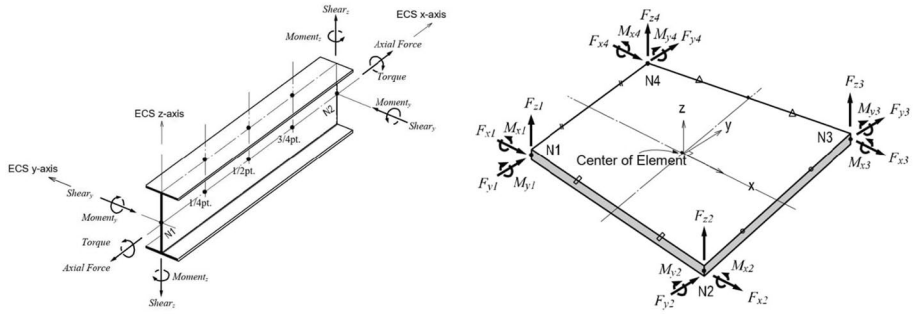

Fig. 4 Elements utilized in the numerical model (**a**) Beam element (**b**) Plate element [21]

Table 3 Number of elements and number of degrees of freedom for the studied buildings for both analyses

Building designation	Mesh size	No. of beam elements for floor beams	No. of beam elements for columns	No. of plate elements for slabs	No. of plate elements for shear walls	No. of degrees of freedom
B_{d1}	Coarse	2400	360	3840	-	25920
	Fine	4800	720	15360	-	100080
B_{d5}	Coarse	-	640	7680	320	51840
	Mesh	-	1280	30720	1280	203520

performance in conducting SA as reported by [10, 11, 22, 23]. Two nodes 3D beam elements (Fig. 4a) are used to model the columns and beams whereas four node 3D plate elements (Fig. 4b) are utilized to simulate the slabs and walls. Each node includes six degrees of freedom (3 displacements and 3 rotations). Rotations are prevented at the between the beam-column and the beam wall connections.

Stiffness is updated at each load step to account for the geometric non-linearity. A bilinear stress–strain relationship is utilized for steel to consider its nonlinear behaviour [21]. The elasto-plastic model of [24] is implemented to consider for the non-linear performance of concrete under compression. The tensile strength for concrete is ignored, according to different comprehensive research work [6–9]. Time-dependent behaviour of concrete is included using the parameters calculated according to [25] code and CEB-FIP [26] standards. More details about the selected parameters can be found in [10].

The *FEM* is validated by conducting *OA* for the six studied *RC* buildings under wind loading using [21] and comparing the results with those obtained from [14] who utilized CSI ETABS software [16] in modelling the same buildings. The *FEM* mesh is adopted in the current study after conducting a sensitivity analysis by modelling buildings B_{d1} and B_{d5} using two different mesh sizes for each building. The number of elements in each mesh is shown in Table 3. Drift and structural period for the two buildings, B_{d1} and B_{d5} from the two mesh sizes are plotted in Fig. 5. For both buildings, the difference between the two meshes does not exceed 3% and 5% for the drift and structural period, respectively.

The *SA* is conducted for the investigated buildings using midas Gen software [21] which is selected based on the recommendation of different researchers [10, 11, 22, 23]. The software conduct accurate analysis based on current theories and numerical

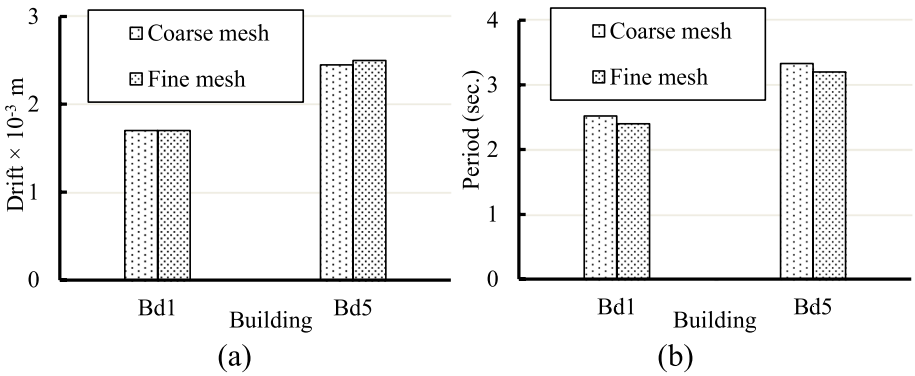

Fig. 5 Results of sensitivity analysis for buildings B_{d1} and B_{d5} (**a**) storey drift (**b**) structural period

Table 4 SA parameters implemented in the model

Activity	Time duration (Day)
Construction cycle	7
Form-work installation	1
Casting of each floor	2
Removal of shoring from lowest level and casting of top floor	5
Member age in each floor	19

methods published in reputable journals. The midas Gen software [21] have been validated by numerous examples and comparisons with other engineering programs. Three consecutive floors are assumed to be supported by form-work in each stage. Table 4 shows the details of adopted *SA* parameters in the developed *FEM*.

Staged-construction analysis methodology

The utilized software, midas Gen [21], accounts for the stages of construction by activating/ deactivating structural elements, boundary conditions, and applied loads. Construction loads are applied to the structural models representing the various construction stages. The flooring and live loads can be applied on a completed building. Only the own weight of the structural elements is considered because live and lateral loads have insignificant effect on *SA* of the building [10]. Figure 6 shows a flowchart summarizing the hybrid analysis steps in midas Gen [21] which includes both *SA* and *OA*. The updated concrete compressive strength is calculated at each time increment based on the time-dependent, according to [27]. Figure 7 shows the construction stages for the *SA* performed for the investigated buildings, as reported by [10]. The time for form-work installation and removal as well as floors casting is provided.

Change in straining actions due to *SA*

Axial loads on columns increases during the construction of a building. Axial deformations of columns lead to redistribution of forces between the columns. Consequently, cracking or severe damage might occur in the structural elements (floors, beams … etc.) and non-structural element (brick walls, curtain walls … etc.). The damages occur due to increase

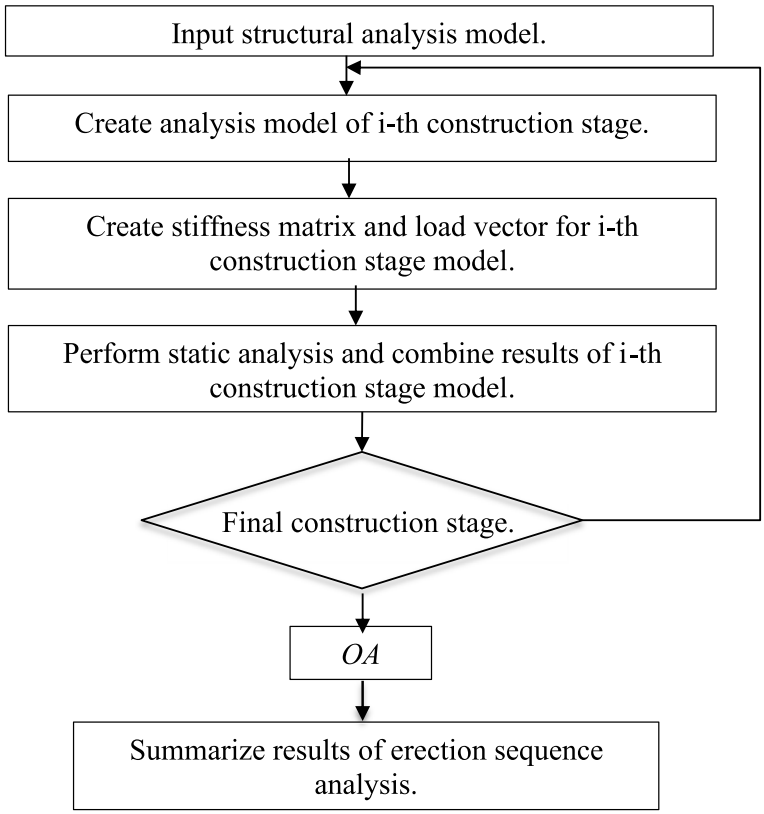

Fig. 6 Erection sequence steps in [21]

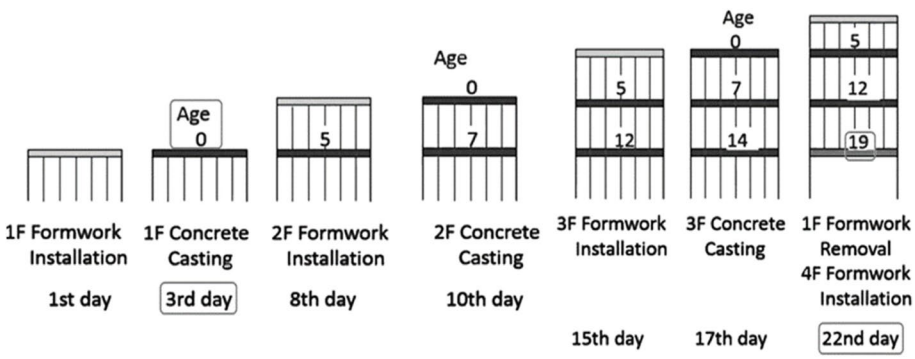

Fig. 7 Construction schedule adopted for *SA* [10]

of internal forces at one end of the beam/slab (Fig. 8). If slabs or beams are analyzed using *OA*, they may experience larger bending moments and shearing forces if re-analyzed using *SA*. Also, the other locations will be over designed where smaller internal forces will be estimated using SA compared to those from *OA*.

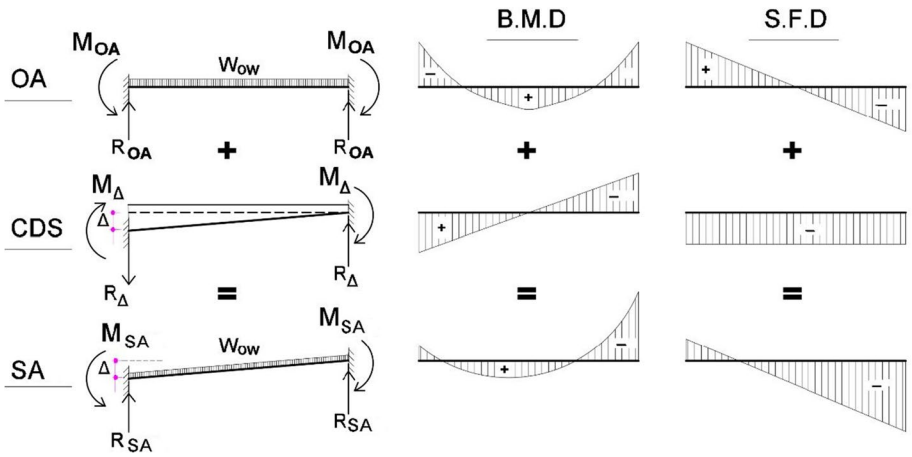

Fig. 8 Bending moments and shearing forces from *OA* and *SA*

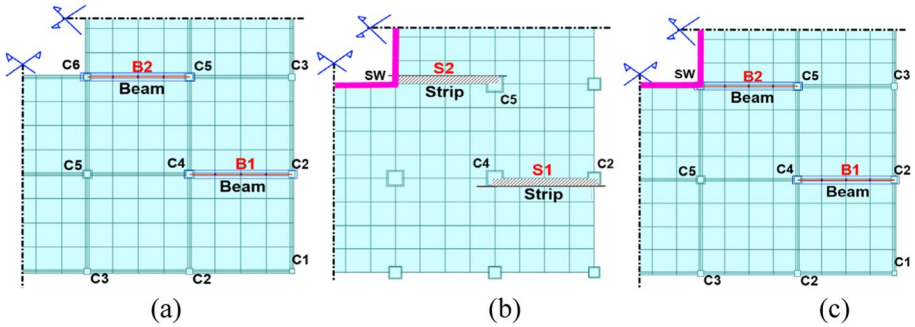

Fig. 9 Plans of studied buildings; (**a**) B_{d1} and B_{d4} (**b**) B_{d2} and B_{d5} (**c**) B_{d3} and B_{d6}

Results and discussion

In this section, the *SSRL* yielding the least differences between deformations and internal forces from *OA* and *SA* for each building height is provided. The differences are obtained from the elements with maximum straining actions: (B1, B2) beams and (S1, S2) strips, as shown in Fig. 9. B1 rests on C2 and C4 columns in buildings B_{d1} and B_{d4} (Fig. 9a) and also in buildings B_{d3} and B_{d6} (Fig. 9c). While B2 rests on C5 and C6 columns in B_{d1} and B_{d4} buildings (Fig. 9a) and supported on column C5 and shear wall SW in buildings B_{d3} and B_{d6} (Fig. 9c). The S1 strip rests on C2 and C4 columns in buildings B_{d2} and B_{d5} (Fig. 9b), whereas S2 strip rests on C5 column and *SW* shear wall in the same buildings. The following equation is utilized to estimate the difference in straining actions from *OA* and *SA*:

$$Diff.\% = \frac{X_{SA} - X_{OA}}{X_{OA,max}} \times 100\% \quad (1)$$

where X_{OA} and X_{SA} are obtained from *OA* and *SA*, respectively.

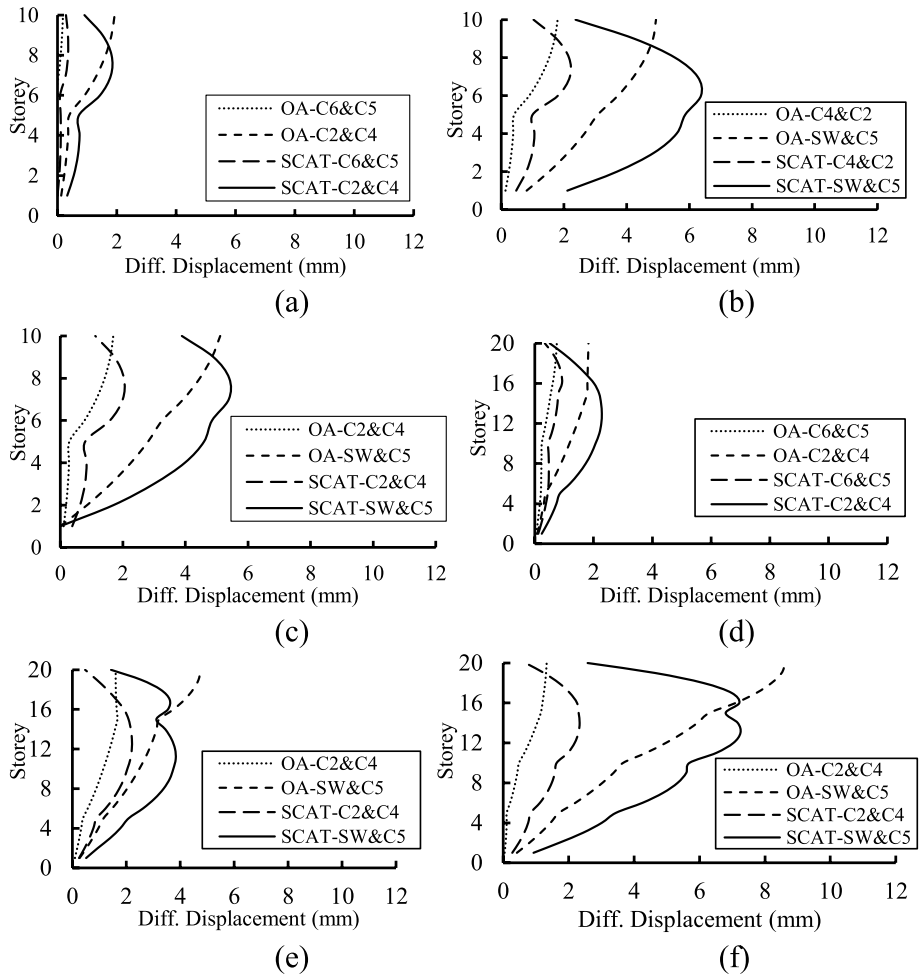

Fig. 10 Differential displacement in columns and walls from *OA* and *SA*: (**a**) B_{d1} (**b**) B_{d2} (**c**) B_{d3} (**d**) B_{d4} (**e**) B_{d5} (**f**) B_{d6}

Differential displacements (DD)

Figure 10 illustrates the *DD* between ends of the considered beams and strips of the slabs where noticeable differences are noted between *OA* and *SA*. *OA* results in a nonlinear distribution for displacements with a maximum value at top of the building. The *SA* also results in a nonlinear *DD* distribution, but the maximum displacement near the mid-height. *OA* yields in a maximum *DD* of 1.92, 4.94, 5.11, 1.83, 4.75, and 8.62 mm for B_{d1} through B_{d6} buildings, respectively (Fig. 10). *SA* yields maximum *DDs* of 1.82, 6.37, 5.40, 2.28, 3.83, and 7.25 for B_{d1} through B_{d6} buildings, respectively. One can observe that buildings B_{d1} and B_{d4} with RF system experienced the minimum *DDs* between beam-ends due to *OA* and *SA*.

Bending moments

Differences between bending moments from *OA* and *SA* are plotted in Fig. 11 for B1 and S1 and in Fig. 12 for B2 and S2. The difference in bending moments noticeably vary because shortenings of vertical elements are not equal. Figure 11 shows that the

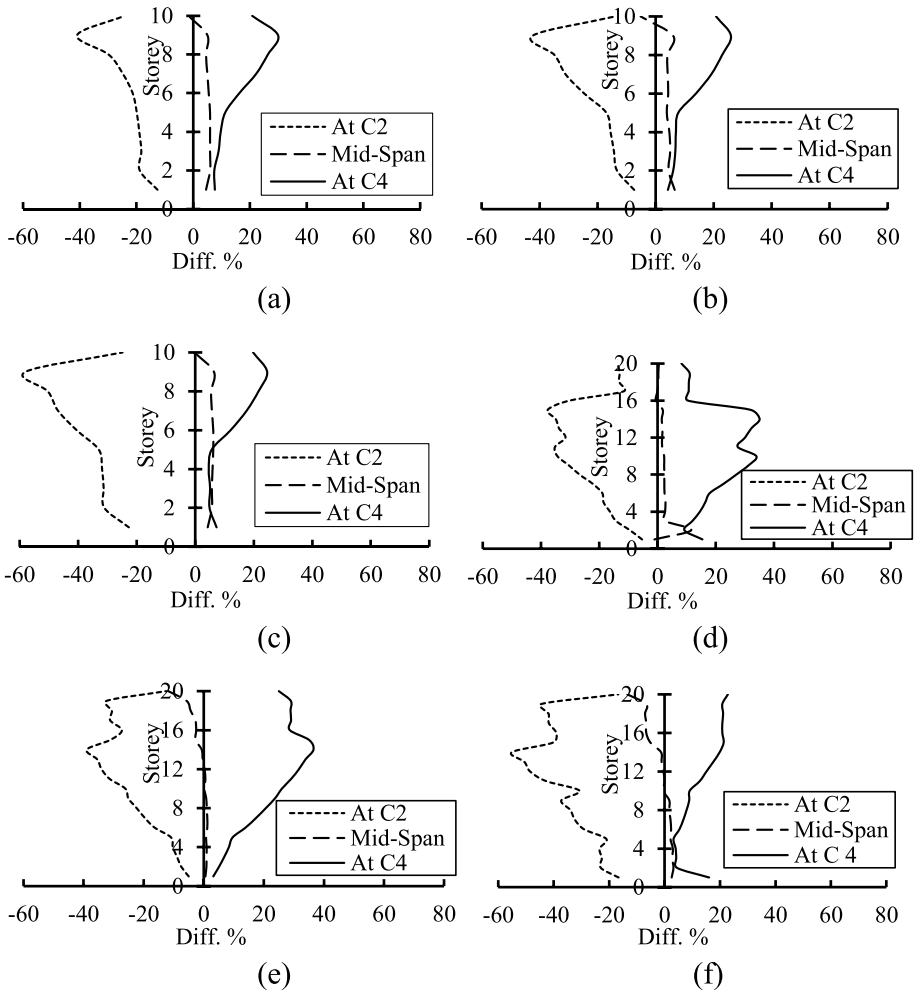

Fig. 11 Difference in bending moments in B1 and S1 between *OA* and *SA*: (**a**) B_{d1} (**b**) B_{d2} (**c**) B_{d3} (**d**) B_{d4} (**e**) B_{d5} (**f**) B_{d6}

bending moments developed in B1 and S1 from *OA* are larger than moments from *SA* by 41.0%, 42.4%, 58.0%, 37.7%, 38.9%, and 55.1% for buildings B_{d1} through B_{d6}, respectively. Same observation can be noted for bending moments in B2 and S2 with percentages of 16.2%, 52.3%, 52.6%, 18.6%, 57.7%, and 62.4% for buildings B_{d1} through B_{d6}, respectively (Fig. 12). Therefore, one can note that *OA* produces an uneconomic design due to utilizing overestimated bending moments. On the other hand, the bending moments from *SA* are higher than those from *OA* by 29.9%, 25.9%, 24.6%, 35.0%, 36.5%, and 22.8% for buildings B_{d1} through B_{d6}, respectively (Fig. 11). Similar trend is observed for the bending moments in B2 and S2 with percentages of 5.7%, 98.4%, 120.9%, 4.4%, 96.3%, and 159.2% for buildings B_{d1} through B_{d6}, respectively (Fig. 12). For buildings B_{d1}, B_{d2}, B_{d3}, and B_{d4}, the *OA* provides underestimated bending moments at the mid-spans. The same trend is noted for lower floors of B_{d5} and B_{d6} and overestimated values are noted at top. However, Fig. 12 depicts that *OA* overestimates the mid-span bending moment of B2 and S2 for buildings B_{d2}, B_{d3}, B_{d4}, B_{d5},

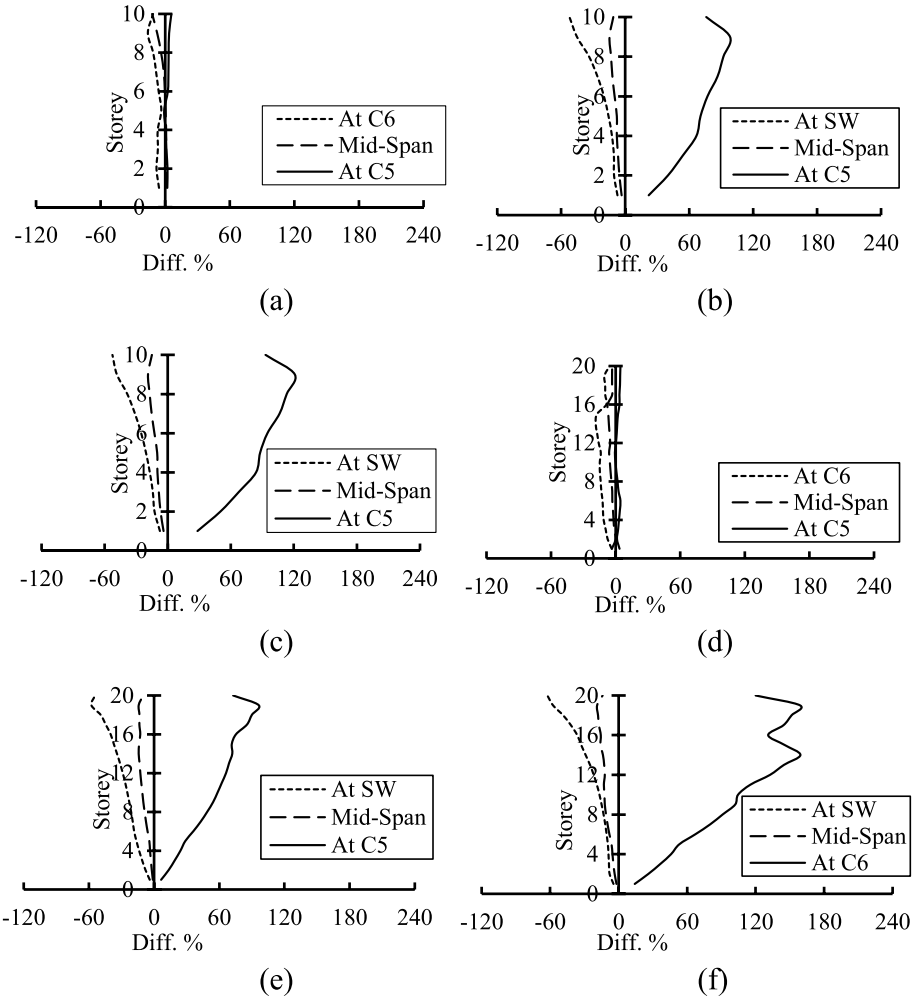

Fig. 12 Difference in bending moment for beam B2 and slab S2 between *OA* and *SA*: (**a**) B_{d1} (**b**) B_{d2} (**c**) B_{d3} (**d**) B_{d4} (**e**) B_{d5} (**f**) B_{d6}

and $B_{d6.}$ The same observation is noted for upper floors of building B_{d1} and underestimated solution is obtained from the *OA* in the lower floors.

Shearing forces

Figures 13 and 14 show the difference in shearing force of beams B1 and B2 from *OA* and *SA* for (B_{d1}, B_{d3}, B_{d4}, and B_{d6}) buildings. The differences in shearing forces dramatically vary along the building height. Maximum difference in shearing forces in B1 from *OA* is higher than those from *SA* by 26.2%, 37.8%, 24.2%, and 35.1% for B_{d1}, B_{d3}, B_{d4}, and B_{d6} buildings, respectively. These percentages for B2 become 11.1%, 49.6%, 14.8%, and 58.9% for buildings B_{d1}, B_{d3}, B_{d4}, and B_{d6}, respectively (Fig. 14). It can be noticed that using *OA* produces uneconomical solution due to utilizing overestimated values. On the other hand, the maximum difference percentage in shearing force for B1 from *SA* is higher than those from *OA* by 19.6%, 13.9%, 23.5%, and 9.3% for B_{d1}, B_{d3}, B_{d4}, and B_{d6}

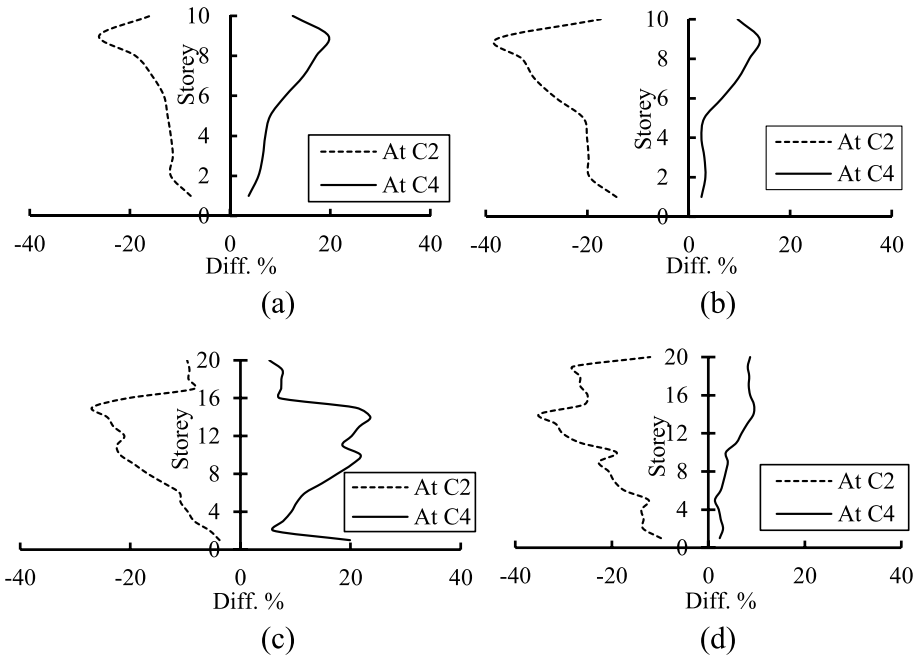

Fig. 13 Difference percentage in shearing force in B1 between *OA* and *SA*: (**a**) B_{d1} (**b**) B_{d3} (**c**) B_{d4} (**d**) B_{d6}

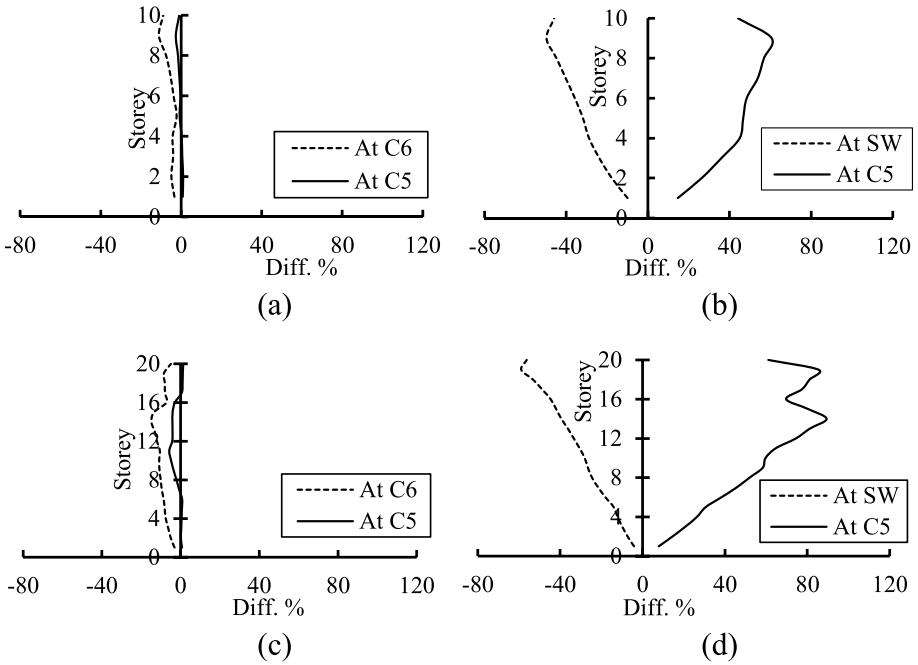

Fig. 14 Difference percentage in shearing force in B2 between *OA* and *SA*: (**a**) B_{d1} (**b**) B_{d3} (**c**) B_{d4} (**d**) B_{d6}

buildings, respectively (Fig. 13). The same note is observed for the maximum shearing force of B2 with percentages of 0.75%, 60.69%, 1.36%, and 89.36% for B_{d1}, B_{d3}, B_{d4}, and B_{d6} buildings, respectively (Fig. 14). Therefore, *OA* yields unsafe design due to utilizing underestimated shearing forces.

Table 5 Maximum *DD* from *OA* and *SA*

Building designation	Maximum *DD* from *OA*, mm	Location (Storey)	Maximum *DD* from *SA*, mm	Location (Storey)	Differences %
B_{d1}	**1.92**	**10**	**1.82**	**8**	**5**
B_{d2}	4.94	10	6.37	6	29
B_{d3}	5.11	10	5.40	8	6
B_{d4}	1.83	20	2.28	13	25
B_{d5}	4.75	20	3.83	11	19
B_{d6}	**8.62**	**20**	**7.25**	**13**	**16**

Table 6 Maximum difference percentage between BMs in beams and slab strips from *OA* and *SA*

Building designation	Maximum percentage % of overestimated *BM*	Storey	Maximum percentage % of underestimated *BM*	Storey
B_{d1}	**41.0**	**9**	**29.9**	**9**
B_{d2}	52.3	10	98.4	9
B_{d3}	58.0	10	120.9	9
B_{d4}	**37.7**	**14**	**35.0**	**14**
B_{d5}	57.7	19	96.3	19
B_{d6}	62.4	19	159.2	14

Table 7 Maximum difference percentage between *SFs* in beams from *OA* and *SA*

Building designation	Maximum percentage % of overestimated SF	storey	Maximum percentage % of underestimated SF	Storey
B_{d1}	**26.2**	**9**	**19.6**	**9**
B_{d3}	49.6	9	60.69	9
B_{d4}	**24.2**	**14**	**23.5**	**14**
B_{d6}	58.9	19	89.36	14

Determining SSRL with minimum difference

The *SSRL* for each building is selected if it produces the smallest difference between maximum differential displacement (*DD*), bending moments (*BM*), and shearing forces (*SF*) from *OA* and SA. Table 5 shows the maximum *DD* between ends of the beams and strips from *OA* and SA. While Tables 5 and 6 show the maximum difference percentage between BM and SF obtained from *OA* and SA for the studied *RC* buildings. Comparing the *DD* of the 10-storey buildings, one can observe that building B_{d1} has the smallest difference in maximum *DD* obtained from *OA* and *SA* (Table 5). The *OA* is noted to provide a maximum *DD* of 1.92 mm at Storey 10, while the SA yield a maximum *DD* of 1.82 mm at Storey 8. Comparing the *DD* of the 20-storey buildings, one can observe that building B_{d6} has the smallest difference in maximum *DD* obtained from *OA* and *SA* (Table 5). The *OA* and *SA* provide a maximum *DD* of 8.62 mm at Storey 20 and 7.25 mm at Storey 13, respectively. Comparing the *BM* and *SF* of the 10-storey buildings, it can be observed that building B_{d1} has the smallest difference between the values obtained from *OA* and *SA* (Tables 6 and 7). The *SA* yields *BM* and *SF* larger than *OA* by 29.9% and 19.6%, respectively both at Storey 9. Similar observations can be noted for building B_{d4} when the BM and SF for the 20-storey buildings are compared. SA resulted in BM and

SF larger than those from *OA* by 35.0% and 23.5%, respectively, both at Storey 14. The observations in this section indicate that RF system provides the minimum difference in *BM* and *SF* between *OA* and *SA* for 10 and 20-storeys buildings.

Conclusions

Analysis of six concrete buildings using Ordinary Analysis (*OA*) and Staged Analysis (*SA*) is conducted in this paper using a robust numerical model which accounts for time dependent effects (*SA*). Moreover, the model accounts for the material and geometric non-linearities. Two different number of storeys (10 and 20) and three various lateral load resisting systems (*RF*, *SW*, and *WF*) are adopted. Differential displacement (*DD*) and straining actions in horizontal elements from the *OA* and *SA* are compared. The following observations can be concluded:

➢ For 10-storeys buildings, maximum *DDs* in beams/slabs using *OA* are 1.92 mm, 4.94 mm, and 5.11 mm for *RF*, *SW*, and *WF* systems, respectively. However, *SA* yields maximum *DDs* of 1.82 mm, 6.37 mm, and 5.40 mm for *RF*, *SW*, and *WF* systems, respectively.

➢ For 20-storeys buildings, the maximum *DDs* in beams/slabs using *OA* are 1.83 mm, 4.75 mm, and 8.62 mm for *RF*, *SW*, and *WF* systems, respectively. However, these differences for *SA* are 2.28 mm, 3.83 mm, and 7.25 mm for *RF*, *SW*, and *WF* systems, respectively.

➢ For 10-storeys buildings, the maximum difference in bending moment in beams obtained from *SA* is larger than those obtained from *OA* by 29.9%, 98.4%, and 120.9% for *RF*, *SW*, and *WF* systems, respectively.

➢ For 20-storeys buildings, the maximum difference in bending moment in beams obtained from *SA* is larger than those obtained from *OA* by 35.0%, 96.3%, and 159.2% for *RF*, *SW*, and *WF* systems, respectively.

➢ For 10-storeys buildings, the maximum difference in shearing force in beams from SA is larger than those from *OA* by 19.6% and 60.7% for *RF* and *WF* systems, respectively.

➢ For 20-storeys buildings, the maximum difference in shearing force in beams from SA is larger than those from *OA* by 23.5% and 89.4% for *RF* and *WF* systems, respectively.

➢ Using *RF* and *WF* systems in 10 and 20-storeys buildings, respectively, provides the minimum difference in *DD* between the *OA* and *SA* analyses. However, the *RF* system yields the minimum difference in straining actions between the *OA* and *SA* analyses for the studied buildings.

It is worth mentioning that the current paper aimed at determining the lateral load resisting system that produce the minimum differences between *OA* and *SA*. This research is currently being extended by examining the seismic behaviour of the investigated buildings.

Abbreviations

OA	Ordinary analysis
SA, SCA	Staged analysis
SCAT	Staged construction analysis considering time-dependent effects

RF	Rigid frame
SW	Shear wall
WF	Wall frame
SSRL	Structural system to resist lateral loads
RC	Reinforced concrete
FE	Finite element
FEM	Finite element model
CFT	Concrete filled tube
DAS	Differential axial shortening
f_c	Concrete characteristic strength
υ_c	Poisson's ratio
E_c	Young's modulus
f_y	Yielding stress
f_u	Ultimate stress
υ_s	Poisson's ratio
E_s	Young's modulus
CDS	Column differential settlement
Diff.%	Difference in straining actions
DD	Differential displacements
BM	Bending moments
SF	Shearing forces

Acknowledgements
The authors would like to thank the Structural Department at the Faculty of Engineering, Cairo University for giving the authors the opportunity to conduct this research work.

Authors' contributions
All authors have read and approved the manuscript. The following shows some details about the contribution of each author. AE: Determined the research point, proposed modelling technique, and criticized the results. AE: Criticized the results, revised the modelling technique, revised the technical writing of the manuscript. MI: Generated the models, wrote the draft of the paper, and implemented the required technical writing revisions.

Funding
The authors declare that no funding was received from any entity to produce the work in this manuscript.

Availability of data and materials
All data utilized to produce this research can be made available upon request.

Declarations

Competing interests
The authors declare that no competing interests are related to the current manuscript.

Received: 1 May 2023 Accepted: 18 June 2023
Published online: 28 June 2023

References

1. Liu NX, Zhao X, Sun HH, Zheng YM, Ding JM (2011) Structural performance assessment and control of super tall buildings during construction. Procedia engineering 14:2503–2510
2. Su J, Xia Y, Xu Y, Zhao X, Zhang Q (2014) Settlement monitoring of a supertall building using the Kalman filtering technique and forward construction stage analysis. Adv Struct Eng 17(6):881–893
3. Fan F, Wang H, Zhi X, Huang G, Zhu E, Wang H (2013) Investigation of construction vertical deformation and pre-deformation control for three super high-rise buildings. Adv Struct Eng 16(11):1885–1897
4. Samarakkody DI, Thambiratnam DP, Chan TH, Moragaspitiya PH (2017) Differential axial shortening and its effects in high-rise buildings with composite concrete filled tube columns. Constr Build Mater 143:659–672
5. Correia R, Lobo PS (2017) Simplified assessment of the effects of columns shortening on the response of tall concrete buildings. Proc Struct Integr 5:179–186
6. Yang WJ, Lee JH, Yi WH (2012) Development of the neural network algorithm for the prediction of column shortening in high-rise buildings. Adv Struct Eng 15(3):509–523
7. Moragaspitiya P, Thambiratnam D, Perera N, Chan T (2010) A numerical method to quantify differential axial shortening in concrete buildings. Eng Struct 32(8):2310–2317
8. Zou D, Liu T, Teng J, Du C, Li B (2014) Influence of creep and drying shrinkage of reinforced concrete shear walls on the axial shortening of high-rise buildings. Constr Build Mater 55:46–56
9. Kwak HG, Kim JK (2006) Time-dependent analysis of RC frame structures considering construction sequences. Build Environ 41(10):1423–1434
10. Elansary A, Mabrouk A, Zawam M, El-Attar A (2022) Staged-Construction Analysis of High-Rise Buildings with Post-tension Slabs. Arab J Sci Eng 47:5281–5302
11. Elansary AA, Metwally MI, El-Attar A (2021) Staged construction analysis of reinforced concrete buildings with different lateral load resisting systems. Eng Struct 242:112535

12. Taranath BS (2009) Reinforced Concrete Design of Tall Buildings (1st ed.). CRC Press, p 989. https://doi.org/10.1201/9781439804810
13. Gunel MH, Ilgin HE (2007) A proposal for the classification of structural systems of tall buildings. Build Environ 42(7):2667–2675
14. El-Leithy NF, Hussein MM, Attia WA (2010) Comparative study of structural systems for tall buildings. J Am Sci 7(4):707-719
15. Katkhoda A, Knaa R (2012) Optimization in the selection of structural systems for the design of reinforced concrete high-rise buildings in resisting seismic forces. Energy Procedia 19:269–275
16. ETABS, CSI (2016) Extended 3D analysis of building systems, Nonlinear V. 16. Computers and Structures, Inc., Berkeley
17. Sap2000, C.S.I (2016) Analysis reference manual. Version 18. Computers and structures, Berkeley
18. Fintel M, Ghosh SK, Iyengar H (1987) Column shortening in tall buildings- Prediction and compensation. Publ. EB108 D Portland Cement Assoc Skokie 3:1–34
19. ACI Committee (2005) Building code requirements for structural concrete (ACI 318-05) and commentary (ACI 318R-05). Technical Documents, Vol 318. ACI report: American Concrete Institute, p 432
20. Structural Engineering Institute (2006) Minimum design loads for buildings and other structures (Vol. 7, No. 5). American Society of Civil Engineers. https://fliphtml5.com/vvkpg/qqsy/basic
21. Technical Specifications of midas Gen. Analysis for Civil Structures 2012:400. http://en.midasuser.com/product/gen_overview.asp
22. Ha T, Lee S (2013) Advanced construction stage analysis of high-rise building considering creep and shrinkage of concrete. Advances in Structural Engineering and Mechanics. pp 2139–47
23. Afshari MJ, Kheyroddin A, Gholhaki M (2018) Simplified time-dependent column shortening analysis in special reinforced concrete moment frames. Periodica Polytechnica Civil Eng 62(1):232–249
24. Mander JB, Priestley MJ, Park R (1988) Theoretical stress-strain model for confined concrete. J Struct Eng 114(8):1804–1826
25. Videla C, Carreira DJ, Garner N (2008) Guide for modeling and calculating shrinkage and creep in hardened concrete. ACI report, ACI Committee 209, p 48. ISBN: 9780870312786
26. CEB FIP Model Code 90, M.C (1990) Comite Euro International du Beton. pp 51–9
27. ACI Committee (2019) Building code requirements for structural concrete (ACI 318-19) and commentary (ACI 318R-19). Technical Documents. American Concrete Institute, p 624. ISBN: 978-1-64195-056-5. https://doi.org/10.14359/51716937

Publisher's Note